

## Inelastic Scattering of Neutrons

E. A. ELIOT, D. HICKS, L. E. BEGHIAN, AND H. HALBAN  
*Clarendon Laboratory, Oxford, England*

(Received December 15, 1953)

Experiments have been carried out on the inelastic scattering of 2.5 Mev neutrons by chromium, bismuth, iron, and indium, using scintillation counters. Inelastically scattered neutrons and gamma rays were observed in a stilbene crystal and the results interpreted by a ratio method. Gamma radiation alone was observed in a sodium iodide crystal, using a normalization technique to eliminate the neutron background.

The following levels were identified: in chromium  $1.42 \pm 0.05$  Mev (cross-section  $1.0 \pm 0.2$  barns); in bismuth  $1.58 \pm 0.05$  Mev ( $0.6 \pm 0.2$  barns) and  $0.85 \pm 0.02$  Mev ( $1.2 \pm 0.3$  barns); and in indium  $0.92 \pm 0.04$  Mev ( $0.4 \pm 0.1$  barns) and  $0.61 \pm 0.06$  Mev ( $0.2 \pm 0.1$  barns). Preliminary experiments with iron gave a level of  $0.91 \pm 0.15$  Mev ( $1.0 \pm 0.3$  barns).

### 1. INTRODUCTION

SINCE the discovery of inelastic scattering of neutrons in 1935<sup>1,2</sup> many attempts have been made to measure the energy distributions and intensities of the scattered neutrons and associated gamma rays. Such measurements should yield valuable information about cross sections and excitation energies of levels in the scattering nucleus, and in some cases (e.g., Bi<sup>209</sup>) the process excites energy levels which have not proved accessible by other methods.

Studies of the process have been made<sup>3</sup> by examination of gamma rays,<sup>4-6</sup> the residual activity of isomeric states,<sup>7</sup> and neutrons.<sup>8-13</sup>

The energy distributions of the gamma rays have been observed for several nuclei<sup>4-6</sup> and the cross sections for inelastic scattering estimated. The disadvantage in observing only gamma radiation is that the excited levels may decay by cascade. This means that the level energies cannot be determined without additional intensity measurements.

In some cases (e.g., In<sup>115</sup>, Au<sup>197</sup>)<sup>7</sup> the levels excited by inelastic scattering may decay into an isomeric state. If the energy of the primary neutrons is gradually increased, there are discontinuities in the intensity of excitation of the isomeric level. Each of these discontinuities corresponds to the excitation of a new level which decays into this isomeric state.

In principle, the most complete information can be derived from the study of neutron groups, since the

energy of each level and the cross section can be determined directly from the energy and intensity of the corresponding group. There are two main experimental difficulties. Firstly, the primary neutrons must be as homogeneous in energy as possible since the scattered groups will have at least the same energy spread as the primary neutrons. Secondly, the inelastically scattered neutrons are of relatively low intensities (less than 5 percent of the primaries in our experiments). The detector must therefore be sufficiently sensitive and at the same time have sufficient resolution to separate the groups. Cloud chambers,<sup>9</sup> proportional counters,<sup>10</sup> photographic plates,<sup>11,12</sup> and organic scintillators<sup>13</sup> have been used as detectors, but the resolution in most cases was not comparable with that of the gamma-ray experiments previously quoted.

In the work described below both neutrons and gamma rays have been observed. The energies of the neutron groups were determined with nearly the same precision as those of the gamma rays. The intensities of the neutron groups were measured with sufficient accuracy to give the cross sections for excitation of each level to between 0.1 and 0.3 barn.

In order to obtain sufficient homogeneity in neutron energy a d-D neutron source was used with a beam energy of 30 kev. With the bad geometry employed this gives a maximum spread of 0.2 Mev in neutron energy.

Since no convenient neutron detector is available which is completely insensitive to gamma radiation, two complementary types of experiment were performed. In the first, both neutrons and gamma rays were observed with a stilbene crystal and photomultiplier. Then the gamma-ray spectrum only was determined with a sodium iodide crystal in place of the stilbene. This made it possible to distinguish the gamma rays from the neutron groups in the spectrum from the stilbene crystal and thus obtain the energy distribution of the inelastically scattered neutrons.

With this technique neutron groups corresponding to the excitation of levels between 0.10 and 2.0 Mev could be observed. Over most of this range resolution of levels more than 0.15 Mev apart appeared to be possible.

<sup>1</sup> D. E. Lea, Proc. Roy. Soc. (London) **A150**, 637 (1935).

<sup>2</sup> Amaldi, D'Agostino, Fermi, Pontecorvo, Rasetti, and Segrè, Proc. Roy. Soc. (London) **A149**, 522 (1935).

<sup>3</sup> H. Goldstein, Nucleonics **11**, 7, 39 (1953).

<sup>4</sup> Beghian, Grace, Preston, and Halban, Phys. Rev. **77**, 286 (1950).

<sup>5</sup> Grace, Beghian, Preston, and Halban, Phys. Rev. **82**, 969 (1951).

<sup>6</sup> R. B. Day, Phys. Rev. **89**, 908 (1953).

<sup>7</sup> A. A. Ebel and C. Goodman, Phys. Rev. **72**, 130 (1951).

<sup>8</sup> B. T. Feld, Phys. Rev. **75**, 115 (1949).

<sup>9</sup> Little, Long, and Mandeville, Phys. Rev. **69**, 414 (1946).

<sup>10</sup> Barschall, Battat, Bright, Graves, Jorgensen, and Manley, Phys. Rev. **72**, 881 (1947).

<sup>11</sup> P. H. Stelson and W. N. Preston, Phys. Rev. **86**, 132 (1952).

<sup>12</sup> Mandeville, Swann, and Seymour, Phys. Rev. **86**, 861 (1952).

<sup>13</sup> M. J. Poole, Phil. Mag. **43**, 1060 (1952).

## 2. NEUTRON SOURCE AND EXPERIMENTAL ARRANGEMENT

The experimental arrangement for the first series of measurements is shown in Fig. 1. The neutrons were produced by the d-D reaction using an occluded target.<sup>4</sup> Disk-shaped scatterers of 5 cm diameter 1 or 1½ cm thick were placed directly in contact with the target. The photomultiplier was placed vertically beneath the scatterer with its window 3 cm from the target. It is evident from the diagram that the inelastically scattered neutrons which could be detected by the stilbene crystal originally left the target in directions between 0° and 90° to the beam direction. With a beam energy of 30 kev these neutrons have primary energies ranging from 2.46–2.67 Mev.

The stilbene crystal (1.5 cm in diameter and 0.5 cm thick) was mounted on an E.M.I. photomultiplier Type VX.5047. Pulses from the photomultiplier were amplified and then analyzed with a 25-channel kick-sorter.

## 3. EXPERIMENTAL PROCEDURE

A number of measurements were made with and without scatterers in position. 20 000–70 000 counts per kick-sorter channel were recorded in each case. The pulse height stability was better than 2 percent. Typical results obtained with chromium are shown in Fig. 2. Although there is evidence of inelastically scattered neutrons, the interpretation of the spectrum is not at all clear. However on taking the ratio for each channel:

$$R = \frac{\text{counts per channel with scatterer}}{\text{counts per channel without scatterer}}, \quad (1)$$

the existence of the group becomes quite clear (see Fig. 6) and its intensity and energy may be calculated as follows.

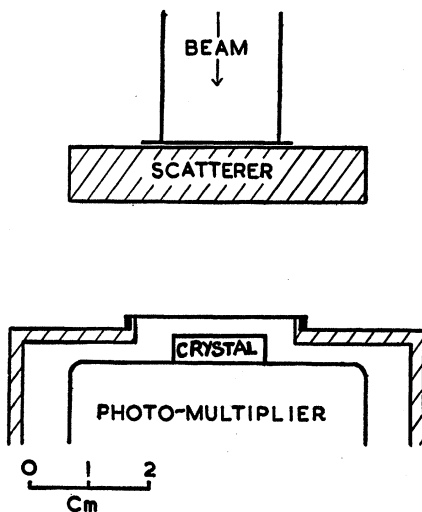


FIG. 1. Experimental arrangement.

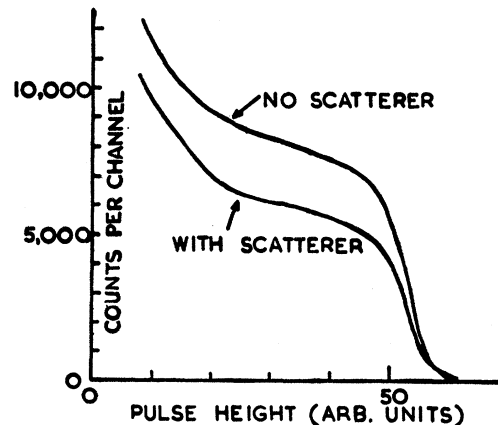


FIG. 2. Pulse-height distributions produced by d-D neutrons in the stilbene crystal taken with and without a chromium scatterer.

## 4. DISCUSSION OF RATIO METHOD

Monoenergetic neutrons in the energy region concerned give rise to a recoil proton spectrum with equal numbers of protons in equal energy intervals. The pulse height  $S$  produced by a recoil proton of energy  $E$  is a unique function of  $E$  (see next paragraph).

Consider the pulse spectrum produced by monoenergetic neutrons. Let  $E_0$  = neutron energy,  $E$  = proton recoil energy ( $E \leq E_0$ ),  $N$  = number of recoil protons produced with energy  $\leq E$ ,  $S$  = pulse height produced by a proton of energy  $E$ . Then,

$$\frac{dN}{dE} = n \quad (\text{where } n \text{ is a constant of the group}). \quad (2)$$

[see Fig. 3(a)];

$$\frac{dN}{dS} = \frac{dN}{dE} \cdot \frac{dE}{dS} = n \frac{dE}{dS}, \quad (3)$$

and  $dN/dS$  is proportional to the counts per channel recorded by the kick-sorter.

With the scatterer in position three types of neutrons enter the crystal, primary, elastically scattered, and inelastically scattered. Since all the materials used were of fairly high atomic mass, elastic scattering produced only a small change in the energy of the neutrons (2 percent for iron and chromium, 1 percent for indium and ½ percent for bismuth). With the resolution available, the recoil spectrum produced by elastically scattered neutrons was indistinguishable from that due to primary neutrons. We shall therefore refer to both these types as "neutrons of full energy."

Suppose for simplicity that a scatterer is used which produces only one group of inelastically scattered neutrons of energy  $E_1$ ; see Fig. 3(b), (c). By analogy with (2) and (3) we have, using primes to denote the presence of the scatterer, for the neutrons of full energy

$$\frac{dN'}{dE} = n', \quad \frac{dN'}{dS} = n' \frac{dE}{dS}; \quad (4)$$

and for the inelastically scattered group

$$d(\Delta N')/dE = \Delta n', \quad d(\Delta N')/dS = \Delta n' dE/dS. \quad (5)$$

Thus taking the ratio  $R$  of counts per kicksorter channel [as in (1) above] we obtain:

(a) when  $S_1 < S < S_0$ ,

$$R = \frac{dN'/dS}{dN/dS} = \frac{n'}{n}; \quad (6)$$

(b) when  $S < S_1$ ,

$$R + \Delta R = \frac{(dN'/dS) + d(\Delta N')/dS}{dN/dS} = \frac{n' + \Delta n'}{n}. \quad (7)$$

A plot of  $R$  against  $S$  will have the form shown in Fig. 3(d).

The pulse height  $S_1$  at the step corresponds to a proton recoil energy equal to that of the inelastically scattered neutrons. The sharpness of the step depends on the homogeneity in energy of the primary neutrons and on the resolution of the photomultiplier. Experimentally obtained ratio plots are shown in Figs. 6, 7. The calculation of cross-sections from these plots depends on the quantity  $\Delta R/R$  (see paragraph 9). This is independent of the actual value of the ratio  $R$ . It was therefore not necessary to normalize the pulse-height distributions taken with and without the scatterer to equal neutron emissions from the source.

The advantages of the ratio method over methods involving subtraction may be summarized as follows: (a) the steps are separated by plateaux; (b) the positions of the plateaux can be fixed with much greater precision than the statistical uncertainty on a single point; (c) it is not necessary to introduce any normalization to reveal the groups; (d) the cross-section calculation is comparatively straightforward though some normalization is needed here (see paragraph 6).

### 5. CALCULATION OF LEVEL ENERGIES

According to Birks<sup>14</sup> the pulse height  $S$  produced in stilbene by a recoil proton of energy  $E$  may be obtained from the following formula

$$\frac{dS}{dr} = \frac{A dE/dr}{1 + kBdE/dr}, \quad (8)$$

where  $r$  = range (centimeters of air) of a proton of energy  $E$ ,  $A$  = a constant of the crystal and electronics, and  $kB$  is a constant obtained in reference (2) from experimental data. Its value is 7.15 Mev/cm air equivalent for anthracene and similar crystals (in particular stilbene).

This formula has been verified for protons of up to

16 Mev.<sup>14</sup> From Eq. (8),

$$S = A \int_0^r \frac{dE/dr}{1 + kBdE/dr} \cdot dr. \quad (9)$$

The integral was evaluated numerically as a function of  $E$  using the range-energy data for protons in air given by Bethe<sup>15</sup> and Bethe and Livingston.<sup>16</sup> Following Birks in reference 2, the variation in stopping power of the crystal with proton energy was neglected. We then have:

$$S = Af(E), \quad (10)$$

where  $f(E)$  is known.

The constant  $A$  was found from the pulse-height distribution measured without scatterer (due to primary neutrons traveling in the beam direction). The pulse height half-way down the fall (see Fig. 2) is taken to correspond to the maximum recoil proton energy of 2.67 Mev. An energy scale is thus established from which the proton recoil energy at any step on the ratio plot may be deduced. This is equal to the energy of the corresponding inelastically scattered neutron group.

The energy of each excited level is calculated by subtracting the energy of the appropriate group from the average primary energy  $\bar{E}_0$  of the inelastically scattered neutrons.  $\bar{E}_0$  is less than the maximum neutron energy of 2.67 Mev because of the variation in energy of the primary neutrons with direction. It was calculated from the geometry of the apparatus and the angular distribution of the d-D neutrons,<sup>17</sup> taking into account only those neutrons which undergo a single inelastic collision. The value of  $\bar{E}_0$  was 2.54 Mev for the 1-cm thick scatterers, and 2.55 Mev for the 1.5-cm thick scatterer. (The upper limit on the error, due to double scattering, was estimated at 0.02 Mev in all cases.)

Gamma rays corresponding to ground state transitions from the levels excited by neutrons have been observed from Cr, Bi, and Fe (see Table I). The agreement between gamma-ray and neutron measurements was within experimental error, which shows that Birks' formula<sup>8</sup> is valid in this energy region.<sup>18,19</sup> However, it is still preferable to deduce excitation energies from gamma-ray measurements, where possible, since these are more precise.

### 6. CALCULATION OF CROSS SECTIONS

The cross section for each inelastic scattering process is calculated from the height of the corresponding step

<sup>15</sup> H. A. Bethe, Revs. Modern Phys. **22**, 213 (1950).

<sup>16</sup> M. S. Livingston and H. A. Bethe, Revs. Modern Phys. **9**, 261 (1937).

<sup>17</sup> Eliot, Roaf, and Shaw, Proc. Phys. Soc. **A216**, 57 (1953).

<sup>18</sup> Allen, Beghian, and Calvert, Proc. Phys. Soc. (London) **A65**, 295 (1952).

<sup>19</sup> In reference 18 the form of the pulse-height distribution was interpreted as indicating that pulse height is proportional to energy. In fact Birks' formula [Eq. (8)] accounts satisfactorily for the observed distribution, especially in the region of proton recoil energy below 1 Mev.

<sup>14</sup> J. B. Birks, Proc. Phys. Soc. (London) **A64**, 874 (1951).

on the ratio plot. Consider the case of the single step represented in Fig. 3.

From Eqs. (6) and (7),

$$\Delta R/R = \Delta n'/n'. \quad (9)$$

Let  $P$  = total number of recoil protons due to neutrons of full energy,  $\Delta P$  = total number of recoil protons due to inelastically scattered neutrons,  $E_0$  = energy of primary neutrons,  $E_1$  = energy of inelastically scattered neutrons,  $M$  = number of neutrons of full energy entering the crystal with scatterer,  $\Delta M$  = number of inelastically scattered neutrons entering the crystal,  $s_0 = n\text{-}p$  scattering cross section for the primary neutrons, and  $s_1 = n\text{-}p$  scattering cross section for the inelastically scattered group. Then

$$\frac{\Delta P}{P} = \frac{\Delta n'}{n'} \times \frac{E_1}{E_0} = \frac{\Delta R}{R} \times \frac{E_1}{E_0},$$

$$\frac{\Delta M}{M} = \frac{s_0}{s_1} \times \frac{\Delta P}{P};$$

therefore

$$\frac{\Delta M}{M} = \frac{\Delta R}{R} \times \frac{E_1}{E_0} \times \frac{s_0}{s_1}. \quad (10)$$

Let  $M_0$  be the number of primary neutrons which would have entered the crystal in the absence of the scatterer (for the same total emission from the source). The ratio  $\Delta M/M$  must be converted to  $\Delta M/M_0$ . To find the conversion factor  $F_1 = M/M_0$ , a series of 1-minute measurements were made alternately with and without scatterer. The total count was recorded above a discriminator bias level set sufficiently high to cut out all pulses due to inelastically scattered neutrons (i.e., pulses were recorded with pulse height greater than  $S_1$ ). Thus, apart from a negligible contribution from high-energy gamma rays (see paragraph 7), all the counts recorded were due to neutrons of full energy.

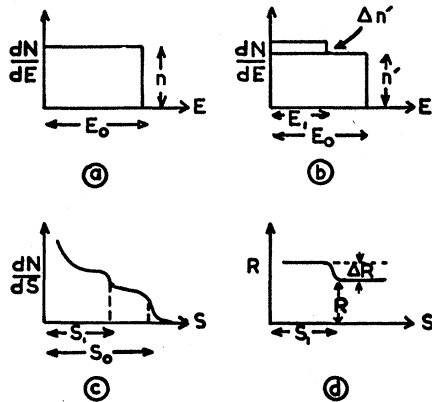


FIG. 3. (a) Energy distribution of recoil protons (no scatterer); (b) energy distribution of recoil protons (with scatterer); (c) idealized pulse-height distribution with scatterer; (d) idealized ratio plot.

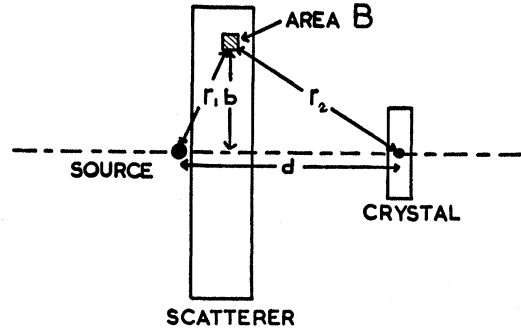


FIG. 4. Notation for cross-section calculation.

Then

$$F_1 = \left( \frac{\text{total count recorded with scatterer}}{\text{total count recorded without scatterer}} \right). \quad (11)$$

For the chromium scatterer  $F_1 = 0.91 \pm 0.01$ , for bismuth  $F_1 = 0.89 \pm 0.01$ , and for indium  $F_1 = 0.98 \pm 0.01$ . Then

$$\frac{\Delta M}{M_0} = F_1 \left( \frac{\Delta M}{M} \right) = F_1 \left( \frac{\Delta R}{R} \right) \left( \frac{E_1}{E_0} \right) \left( \frac{s_0}{s_1} \right). \quad (12)$$

The relation between the inelastic scattering cross section and  $\Delta M/M_0$  is calculated by dividing the scatterer into a number of rings of square cross section (see Fig. 4). In assessing the contribution by inelastic scattering of each ring to  $\Delta M/M_0$ , the following assumptions were made:

- (1) The neutron flux emitted from the target has an angular distribution of the form  $(1 + A \cos^2\theta)$ , where  $A = 0.5 \pm 0.1$  at 30 keV,<sup>17</sup> and  $\theta$  is the angle between the neutron path and the beam direction.
- (2) Only those neutrons which undergo a single inelastic collision (and no other processes) need to be considered; i.e., the effect of multiple processes can be ignored.
- (3) The angular distribution of inelastically scattered neutrons is isotropic.

On this basis,

$$\frac{\Delta M}{M_0} = \sigma_i \frac{d^2 N B}{2(1+A)} \sum T \frac{b}{r_1^2 r_2^2} (1 + A \cos^2\theta), \quad (13)$$

where the summation is made over all elements in the scatterer and  $N$  = number of scattering nuclei per unit volume,  $A = 0.5$  (see assumption 1),  $B$  = area of cross section of ring,  $\sigma_i$  = inelastic scattering cross section of scatterer, and  $dr_1 r_2 b$  are distances marked in Fig. 4.

$T$  is the probability that a neutron will undergo no process in its passage through the scatterer other than a single inelastic collision in the volume element concerned. It was calculated from total neutron cross sections of the scattering material.

Combining Eqs. (12) and (13) yields:

$$\sigma_i = \frac{F_1 \left( \frac{\Delta R}{R} \right) \left( \frac{E_1}{E_0} \right) \left( \frac{s_0}{s_1} \right)}{\left\{ \frac{d^2 N}{2(1+A)} \sum T \frac{b}{r_1^2 r_2^2} (1+A \cos^2 \theta) \right\}} \quad (14)$$

Assumption (2) is only true as a first approximation and will cause the value of  $\sigma_i$  deduced from Eq. (14) to be too high, since there are also contributions to  $\Delta M/M_0$  from multiple processes. Corrections were estimated from the total neutron cross sections and the value of  $F_1$ . The increases in  $\sigma_i$  were found to be

- (12±10) percent for bismuth,
- (8±7) percent for chromium,
- (2±2) percent for indium.

The total neutron cross section for chromium at 2.5 Mev is not known. A value of 3 to 5 barns seems reasonable for an element of this atomic mass. The extreme values of the correction are then (4±4) percent and (12±10) percent. The value quoted above corresponds to a cross section of 4 barns. No correction has yet been calculated for iron since the measurements are still in the preliminary stage.

Even if assumption (3) is not valid and the angular distribution of scattered neutrons is markedly anisotropic, the value calculated for the cross section will not be much in error because of the poor geometry. Consider for example the hypothetical case:<sup>20</sup>

Target nucleus	$I = \frac{1}{2}$ ,
Compound nucleus	$J = 3$ ,
Product nucleus	$I' = \frac{3}{2}$ ,
Incident neutron	$l = 2$ ,
Scattered neutron	$l' = 1$ ,

where the angular distribution is

$$W(\phi) = 1 + \frac{36}{23} \cos^2 \phi.$$

( $\phi$  is the angle between the paths of the incident and scattered neutrons.)

In this case calculation of the cross section on the assumption that the distribution is isotropic leads to a value which is 4 percent too low.

#### 7. RESPONSE OF THE STILBENE CRYSTAL TO GAMMA RAYS

The detection efficiency of the crystal for gamma rays of mean energy 1.25 Mev from a standard Co<sup>60</sup> source was measured and found to be 4 percent. This is

<sup>20</sup> E. Segrè, *Experimental Nuclear Physics* (John Wiley and Sons, Inc., New York, 1953), Vol. II, p. 300.

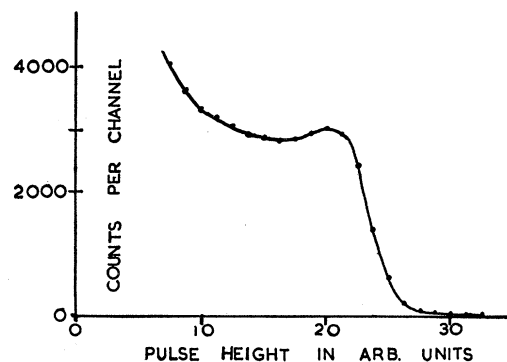


Fig. 5. Pulse-height distribution produced in the stilbene crystal by the 810-keV gamma rays from Mn<sup>54</sup>.

comparable to the 5 percent efficiency for 2.5-Mev neutrons calculated from the  $n-p$  cross section. Moreover, Compton electrons and recoil protons give rise to similarly shaped pulse-height distributions (compare Figs. 2 and 5), so that gamma rays as well as neutrons can produce steps on the ratio plot. The pulse height at the Compton edge of a 0.9-Mev gamma ray is equal to that of a 2.5-Mev recoil proton. Thus each step may be provisionally interpreted either as a neutron group corresponding to a certain level excitation or as a gamma ray of some definite energy less than 0.9 Mev. So that a final interpretation of the ratio plot might be obtained, the gamma-ray energies were investigated in a second series of experiments (see paragraph 8).

Gamma rays of energy greater than 1.1 Mev produce Compton edges beyond the steep fall of the proton recoil spectrum. When a pulse-height distribution is taken with scatterer, these edges can be seen superimposed on a background provided by the high-energy tail of the proton recoil spectrum. This background is predominantly due to the neutrons of full energy. Hence it can be determined from a pulse-height distribution made without scatterer, normalized to the same number of neutrons of full energy, i.e., to the same number of counts per channel on the shoulder of the proton recoil spectrum. Examples of the results obtained are shown in Fig. 6 (curve marked difference plot) and Fig. 8.

#### 8. DETERMINATION OF THE GAMMA-RAY SPECTRUM WITH A SODIUM IODIDE CRYSTAL

In each case investigated, the gamma-ray intensity was only a few percent of that of the primary neutrons. A NaI(Tl) crystal (1-in. cube) was therefore used as the detector, since it is about ten times more sensitive to gamma rays than to neutrons in the energy regions concerned.<sup>21</sup> Even so the neutrons gave rise to a background one to four times the effect of the gamma rays. Since only a small fraction of the neutrons were inelastically scattered, this background was predominantly due to neutrons of full energy. Accordingly it could be

<sup>21</sup> M. A. Grace (private communication).

calculated from a primary neutron pulse-height distribution taken without the scatterer.

Two pulse-height distributions were recorded, *A* with and *B* without the scatterer. These were normalized to the same total neutron emission from the source. Then the ratio  $F_3$  of the numbers of neutrons of full energy detected with and without the scatterer was found with a stilbene crystal, by a method similar to that used for  $F_1$  (see paragraph 6). The background in the gamma-ray measurement (*A*) could now be found by multiplying the counts in each channel of (*B*) by the factor  $F_3$ .

When measuring  $F_3$ , in order to approximate to the geometry of the sodium iodide crystal, a stilbene crystal 2.5 cm in diameter and 0.5 cm thick was placed successively in positions corresponding to the top and bottom of the one-inch cube. A value of  $F_3$  was found for each position, and the mean value weighted with respect to counting rate was calculated. For the bismuth scatterer  $F_3 = 0.88 \pm 0.01$  and for indium  $F_3 = 0.98 \pm 0.01$ . No sodium iodide measurements have been made with

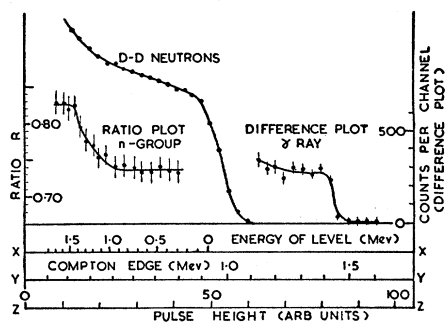


FIG. 6. Chromium. Neutron group and associated gamma ray observed with the stilbene crystal.

chromium or as yet with iron (see "Discussion of Results").

A gamma-ray spectrum obtained after subtracting the neutron background is shown in Fig. 9, which refers to bismuth. The apparently poor resolution is due to the degradation of the gamma rays in their passage through the scatterer. For the purpose of checking this, pulse-height distributions of 0.81-Mev ( $\text{Mn}^{54}$ ) and 1.28-Mev ( $\text{Na}^{22}$ ) gamma rays were recorded with the scatterer interposed between source and detector. The results obtained were very similar to Fig. 9. This similarity also justifies the assumption that any background due to inelastically scattered neutrons can be neglected.

## 9. DISCUSSION OF RESULTS

### Chromium (Fig. 6)

The scattering material consisted of chromium filings contained in a cylindrical can of aluminium 5 cm diameter  $\times$  1 cm deep and 0.03 cm thick. The results obtained are shown in Fig. 6. The curve marked D-D

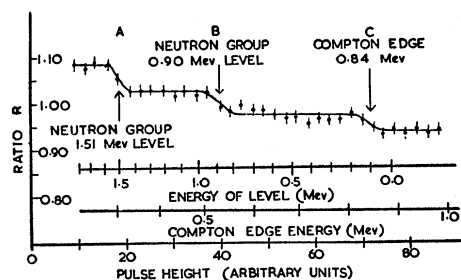


FIG. 7. Bismuth. Ratio plot.

neutrons shows the pulse-height distribution due to primary neutrons on an arbitrary vertical scale. The single step found on the ratio plot represents a scattered neutron group associated with a level of  $1.3 \pm 0.1$  Mev or, alternatively, gamma radiation of 0.4 Mev. The Compton edge of a gamma ray of  $1.42 \pm 0.05$  Mev was found beyond the neutron spectrum (see curve marked difference plot) in agreement with the work of Grace *et al.* using a sodium iodide crystal.<sup>22</sup> It was therefore not considered necessary to make sodium iodide measurements in this case. Since there were no other steps on the ratio plot and since some level must have been excited to give the 1.4-Mev gamma ray, we interpreted the step found as a neutron group. The cross section was calculated from the height of the step and was  $1.0 \pm 0.2$  barns.

### Bismuth (Figs. 7, 8, 9)

The scatterer was a cylindrical block 5 cm diameter by  $1\frac{1}{2}$  cm thick. Three steps *A*, *B*, and *C* were observed on the ratio plot (Fig. 7). The following alternative interpretations could be made:

Step	Energy of level if a neutron group	Energy if gamma radiation
<i>A</i>	$1.51 \pm 0.10$ Mev	$0.31 \pm 0.03$ Mev
<i>B</i>	$0.90 \pm 0.07$ Mev	$0.53 \pm 0.04$ Mev
<i>C</i>	$0.11 \pm 0.05$ Mev	$0.84 \pm 0.03$ Mev

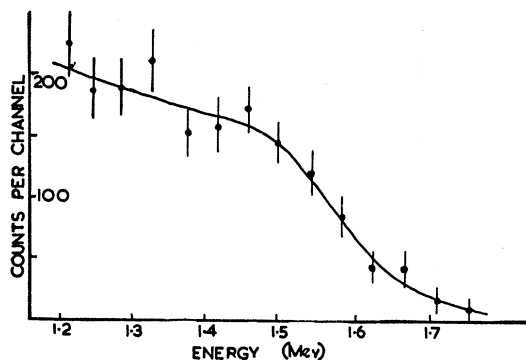


FIG. 8. Bismuth. Compton edge of 1.58-Mev gamma ray observed with the stilbene crystal.

<sup>22</sup> Grace, Lemmer, and Halban, Proc. Phys. Soc. (London) A65, 456 (1952).

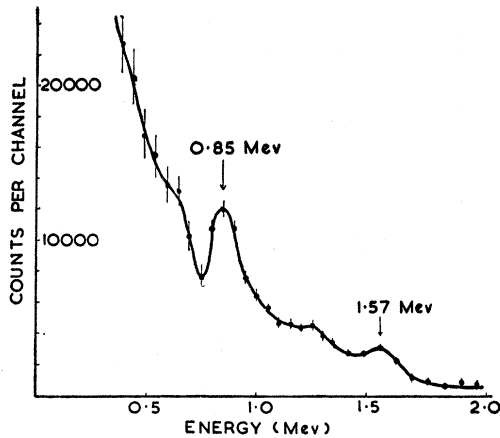


FIG. 9. Bismuth. Gamma rays observed with sodium iodide crystal.

The Compton edge of a gamma ray of  $1.59 \pm 0.05$  Mev was also observed with the stilbene crystal (Fig. 8).

With the sodium iodide crystal two gamma rays were observed (Fig. 9):

$0.85 \pm 0.03$  Mev and  $1.57 \pm 0.07$  Mev.

The results were interpreted as follows. Step C corresponds to the 0.85-Mev gamma ray observed with the sodium iodide crystal. The presence of this radiation and the absence of a 0.53-Mev gamma ray in the sodium iodide measurements shows that step B must be a neutron group. Considering step A, the possibility of a 0.31-Mev gamma ray cannot be ruled out on the evidence of Fig. 9 alone. If A is due to gamma radiation, then it must correspond to a transition to the ground state or to the 0.85-Mev level. Thus a neutron group would be required to feed a 0.31-Mev or a 1.19-Mev level. No steps of the necessary intensity are observed at either energy (see Fig. 7). Therefore A must represent

a neutron group. This conclusion is supported by the presence of the 1.58-Mev gamma ray.

Our final interpretation is that two levels of energies  $1.58 \pm 0.05$  Mev and  $0.85 \pm 0.02$  Mev are excited with cross sections of  $0.6 \pm 0.2$  and  $1.2 \pm 0.3$  barns, respectively, and each decays directly to the ground state.

The possibility that the 1.58-Mev level also decays by cascade through the 0.85-Mev level with the emission of 0.73-Mev gamma ray cannot be excluded. (Upper limit to intensity 30 percent of the 1.58 Mev ground-state transition.)

### Indium

Six steps were observed on the ratio plot (Fig. 10). The following alternative interpretations could be made:

Step	Energy of level (Mev) if a neutron group	Energy (Mev) if a gamma ray
A	$1.70 \pm 0.05$	$0.23 \pm 0.03$
B	$1.36 \pm 0.05$	$0.35 \pm 0.03$
C	$1.14 \pm 0.05$	$0.43 \pm 0.03$
D	$0.92 \pm 0.04$	$0.52 \pm 0.03$
E	$0.61 \pm 0.06$	$0.64 \pm 0.04$
F	$0.25 \pm 0.07$	$0.75 \pm 0.05$

Gamma rays of the following energies (Mev) were observed with the sodium iodide crystal:

$0.25 \pm 0.03$ ,  $0.34 \pm 0.02$  (isomeric),  
 $0.44 \pm 0.03$ ,  $0.87 \pm 0.03$ .

Unresolved gamma rays between 1.1 and 2 Mev were observed with both crystals. The possibility of a 0.75-Mev gamma ray in the spectrum obtained with the sodium iodide crystal cannot be excluded. The decay of the isomeric state was observed after the neutron bombardment had ceased

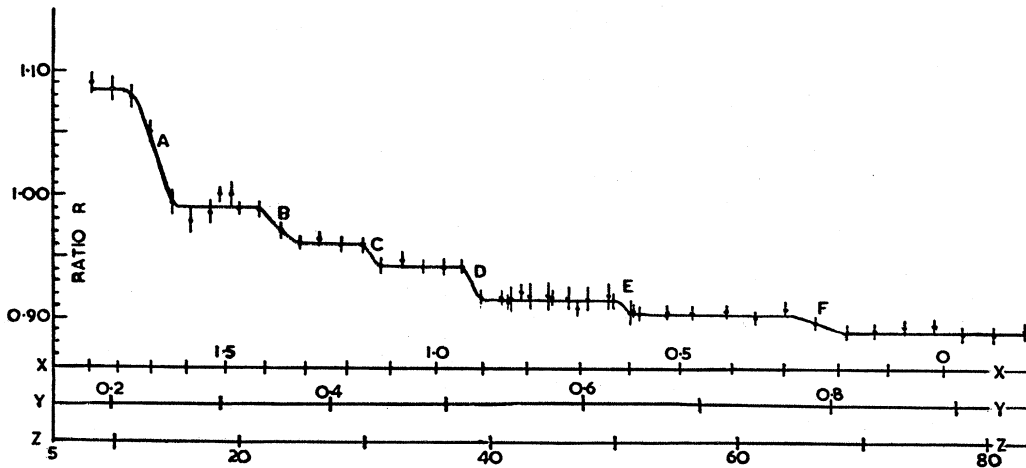


FIG. 10. Indium. Ratio plot.

Scale X—Energy of level excited by neutrons (Mev).  
Scale Y—Gamma ray Compton edge (Mev).  
Scale Z—Pulse height (arbitrary units).

Our tentative interpretation of these results is

Step *A*:  $\gamma$  ray.

Step *B*:  $\gamma$  ray (but see below).

Step *C*:  $\gamma$  ray.

Step *D*: Neutron group—level excited  $0.92 \pm 0.04$  Mev;  
cross section  $0.4 \pm 0.1$  barn.

Step *E*: Neutron group—level excited  $0.61 \pm 0.06$  Mev;  
cross section  $0.2 \pm 0.1$  barn.

Step *F*: Probably a weak  $\gamma$  ray.

There was no trace of direct excitation of the 360-kev isomeric level; from the ratio plot the upper limit to this cross section is 0.1 barn.

These results are in agreement with those of Ebel and Goodman<sup>7</sup> from excitation of the isomeric state. They found levels in In<sup>115</sup> at

$0.60 \pm 0.04$  Mev,  $0.96 \pm 0.04$  Mev,  $1.37 \pm 0.04$  Mev.

The neutron group corresponding to a 1.37-Mev level would produce a step on the ratio plot which could not be resolved from that due to the isomeric gamma ray. The cross section for excitation of the 1.37-Mev level cannot therefore be deduced from our results.

### Iron

Preliminary experiments showed a single step on the ratio plot which can be interpreted as a neutron group

TABLE I. Summary of results.

Nucleus	Energy of level from neutron group (Mev)	Cross-section barns	Energy of gamma ray	
			from stilbene Mev	from NaI Mev
Chromium	$1.30 \pm 0.10$	$1.0 \pm 0.2$	$1.42 \pm 0.05$	
Bismuth	$1.51 \pm 0.15$	$0.6 \pm 0.2$	$1.59 \pm 0.05$	$1.57 \pm 0.07$
	$0.90 \pm 0.10$	$1.2 \pm 0.3$	$0.84 \pm 0.03$	$0.85 \pm 0.03$
Iron (preliminary result)	$0.91 \pm 0.15$	$1.0 \pm 0.3$		
Indium	$0.61 \pm 0.06$	$0.2 \pm 0.1$	No ground state $\gamma$ observed	No ground state $\gamma$ observed
	$0.92 \pm 0.04$	$0.4 \pm 0.1$	No ground state $\gamma$ observed $0.23 \pm 0.03$ $0.35 \pm 0.03$ $0.43 \pm 0.03$	No ground state $\gamma$ observed $0.25 \pm 0.03$ $0.34 \pm 0.02$ $0.44 \pm 0.03$ $0.87 \pm 0.03$

from a level of  $0.91 \pm 0.15$  Mev, in agreement with previous work.<sup>4,6</sup>

The results for chromium, bismuth, iron, and indium are summarized in Table I.

We would like to thank Dr. D. Roaf and Dr. P. F. D. Shaw for the use of the high-tension set and Dr. D. J. Hughes for his helpful criticism of the manuscript. We also wish to thank Lord Cherwell for extending to us the facilities of this laboratory.